Astronomy & Astrophysics manuscript no. main
September 2, 2014

Nickel mass estimates of Type Ia Supernovae from NIR data: Test case for SN2014J and SN2006X

TBD

[1] European Southern Observatory, Karl Schwarzschild Strasse 2, Garching bei Munchen, Germany, 85748
e-mail: @eso.org
[2]

Preprint online version: September 2, 2014

Abstract

Aims. To determine the relation between the amount of Nickel produced in SNIa and the timing of the second maximum and to extrapolate Nickel mass values for highly reddened SNIa using this relation
Methods. We measure the (pseudo)-bolometric luminosity at peak and use it to derive a value of M_{Ni} mass for a 'low-reddening' sample of objects from the literature in order to minimize effects from presuming a reddening law.
Results. We find a strong correlation between the M_{Ni} and t_2 in the Y and J bands and a weaker trend in the H band. We use this empirical relation to derive M_{Ni} for two test case SN with high extinction (> 1.2 mag). This allows us to have a M_{Ni} value which is independent of the reddening law applied.
Conclusions. From our results we conclude that an empirical relation between M_{Ni} and t_2 can allow us to infer the M_{Ni} for highly reddened objects without an estimate of their total absorption. The results for SN2014J from this method correspond well with the values obtained from recent γ ray observations, thus providing further evidence of the potency of this technique

Key words. stars: supernovae: general

1. Introduction

Type Ia supernovae (SNe Ia) have been used as cosmological distance indicators and have provided first evidence for the accelerated expansion of the universe (**??**). . Their potency as cosmological probes has led to dedicated efforts to understand the nature of these explosions to reduce effects from systematics in the constraints of the cosmological parameters.

SNIa in the optical, however, require corrections using correlations between observables (**??**) to improve cosmological parameter estimation. Recent studies of SNeIa have indicated that the SNIa are much more uniform in .

Observations of large samples of SNe Ia show that the peak luminosity in the optical is not uniform (e.g. **??????**), leading to different bolometric luminosities for the objects (**?**) implying variations in the physical parameters of the explosion, in particular the synthesised nickel mass and the total ejected mass (**??**). The correlation at optical wavelengths between peak luminosity and light curve shape together with the determination of the absorption towards the supernova are the key ingredients of the calibration of these objects prior to their use as distance indicators (**?**).

At near infrared wavelengths SNeIa display a very uniform brightness behaviour (**????**). The scatter in the peak luminosity in these studies is 0.2 magnitudes, which, combined with the lower sensitivity of the IR to extinction by dust, has sparked increased interest in this wavelength region. Statistically significant samples of SN Ia light curves are thus becoming available (**????**) and have been used to construct the first rest-frame near-infrared Hubble diagrams (**????**).

The light curve morphology in the infrared is markedly different from that in the optical, with a pronounced secondary maximum in $IYJHK$ filters for 'normal' SNe Ia and a 'shoulder' in the V and R filter light curves (**??????**). **?** demonstrated that the second maximum could be the result of decrease in opacity due to the ionization change of Fe group elements from doubly to singly ionized atoms, which preferentially radiate the energy at near-IR wavelengths. He further indicated that larger iron mass would lead to a later maximum in the NIR light curves.

Recent studies have shown a strong dependence of the timing of the second maximum (hereafter t_2) on the decline rate of the SNIa, indicating that brighter explosions have a later onset of the second maximum. A strong relation between the t_2 and the onset of the uniform optical colour phase (hereafter t_L, see also t_{max} **?**) suggests that the second maximum is related to the colour evolution which is tied to the amount of iron group elements synthesized in the explosion (**?**). The conclusion from these studies point to a connection between the $M_{^{56}Ni}$ in SNIa and t_2.

In this study, we investigate ,directly, the link between the $M_{^{56}Ni}$ and t_2. We use a sample of nearby objects with low extinction from dust, in order to circumvent uncertainties from the specific reddening law used. We aim to use this relation to derive $M_{^{56}Ni}$ for heavily extinguished SNae where using the bolometric peak is extremely sensitive to the total absorption value used, and hence, the reddening law. To this end, we propose using NIR only data at late times along with an empirical relation to obtain precise estimates of $M_{^{56}Ni}$ for objects where other methods provide disparate results.

Send offprint requests to: TBD

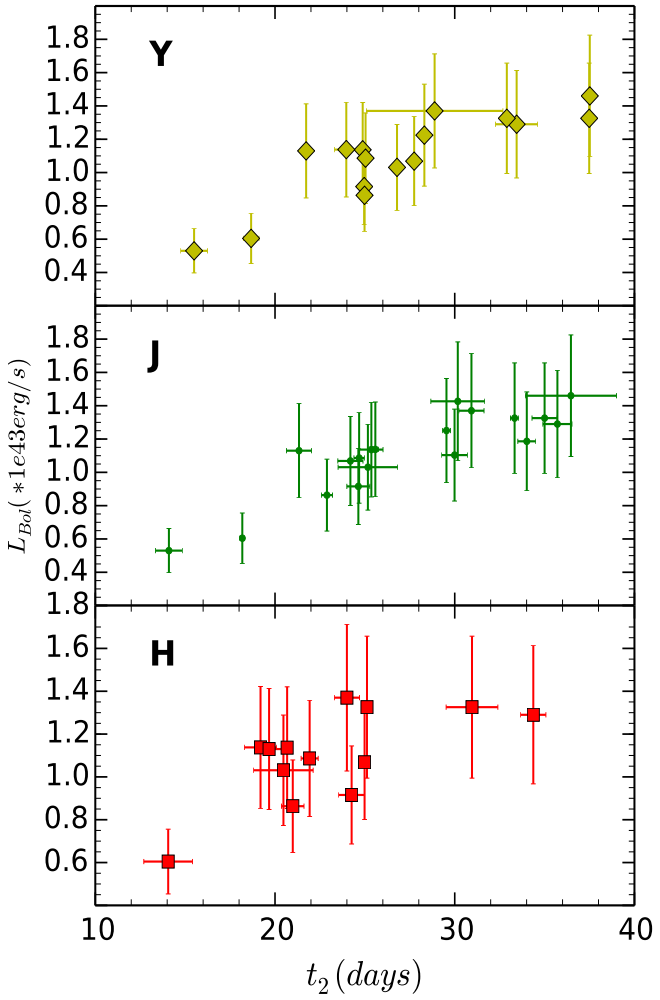

Figure 1. L_{max} is plotted against the t_2 in YJH bands. A strong correlation is observed in the Y and J, whereas a weaker correlation is seen in the H band. **this only includes objects with a u-H measured bolometric peak and not any of the others**

2. Data

The sample for this study is constrained by objects which have NIR observations at late times as well as well-sampled optical light curves to construct a (pseudo-) bolometric light curve. The main data source of near-infrared photometry of SNe Ia currently comes from the Carnegie Supernova Project (CSP; **?????**). They form an ideal basis for an evaluation of light curves parameters. We add to this sample objects from the literature and the nearby objects SN2011fe.

Since we aim to circumvent the uncertainties from host galaxy extinction, we only select objects with an $E(B-V)_host$ value less than 0.1. Since we want to investigate the connection of M_{Ni} with t_2 in the NIR, this excludes objects which are spectroscopically similar to the peculiar SN 1991bg (**???**) and objects that do not exhibit a second maximum (SNe 2005bl, 2005ke, 2005ku, 2006bd, 2006mr, 2007N, 2007ax, SN2007ba, 2009F). On similar lines we exclude peculiar objects like 2006bt and 2006ot. These constraints leave us with a final sample of 22 objects.

3. Analysis

The flux emitted by an SNIa in the UV, optical and NIR traces the radiation converted from the radioactive decays of newly synthesized isotopes. As the SN emits most of its flux in the UV to NIR passbands, the "uvoir bolometric flux" represents a physically meaningful quantity (**?**)

We select a low-reddening sample so that our measurements are less sensitive to a reddening law. For objects with sufficient amount of near maximum data in the optical and the NIR, we construct UBVRIJH bolometric light curves. We do not use K band data since there are very few objects in the sample with well-sampled K band light curves. For objects with well-sampled K light curves we calculate the flux emitted in the K band and find that it is between $1-3\%$, thus, not using the K-band is not a dominant source of uncertainty. The magnitudes were corrected for reddening using a CCM reddening law for each filter. The values for the extinction are presented in table 2. The uncertainty in the reddening estimate was propagated into the calculation of the bolometric flux Using zero-points in the given filters, the magnitudes were converted to fluxes. The resulting light curve, in ergs/cm^2/s was converted into an absolute bolometric light curve by using the distances of the SN derived from the host galaxy redshift.

Since all distances are scaled to an $H_0 = 70 kms^{-1}Mpc^{-1}$the errors in the luminosity distance are only affected by the relative errors in the distance moduli (see Table 2 for values and uncertainty estimates). For objects not in the hubble flow, we use distance measurements from published estimates (which use others methods eg. Cepheid, Tully-Fisher relation etc.).

The bolometric light curves were interpolated using a cubic spline. In order to get an $L_{Bol}(max)$ we required sampling in the individual bands at pre-maximum epochs. Thus, for objects without NIR coverage before B_{max}, we use the UBVRI light curves. The errors on the peak were calculated from the errors in the fluxes of the bolometric maximum using a Monte Carlo for 1000 realisations of the light curve.

For objects with no NIR coverage near maximum, we apply a correction like in **?** and increase the M_{Ni} value by 1.1. In **?**, the authors found that using a UVOIR light curve with the correction for the NIR, Arnett's rule estimates the M_{Ni} to $\leq 0.05\ M_\odot$.

4. Results

In this section we present the results derived from the measurements of the peak bolometric luminosity and the trends observed with other observables for the SNe in our low-reddening sample, as well as the complete sample of objects with a measured timing of the second maximum

4.1. Correlation between L_{max} and t_2

In figure 1, we find that there is a very strong correlation between t_2 and M_{Ni} in the Y and J bands with r values of 0.80, 0.88. A much weaker trend is observed in the H band with $r \sim 0.60$. This is reflected in the ratio of the slope to the slope error in equation (1)

In the Y and J band, a strong correlation suggests that objects with more Ni produced show later second maxima.

$$L_{Max} = 0.040(\pm0.005) * t_2(Y) - 0.055(\pm0.125) \quad (1a)$$

$$L_{Max} = 0.042(\pm0.004) * t_2(J) - 0.039(\pm0.102) \quad (1b)$$

Table 1. The sample of SNe which have low reddening, as defined in the text. The references for the data are presented along with the extinction values and the distanes used to calculate the bolometric light curves **to add: distance modulus values**

SN	μ	e_μ	$E(B-V)_{host}$	$E(B-V)_{MW}$	Filters
SN2008gp	0.66	0.14	0.098(0.022)	0.104(0.005)	UBVRIJH
SN2007as	0.44	0.05	0.050(0.011)	0.123(0.001)	UBVRI
SN2008bc	0.68	0.19	< 0.019	0.225(0.004)	UBVRIJH
SN2008hv	0.49	0.13	0.074(0.023)	0.028(0.001)	UBVRIJH
SN2008ia	0.6	0.14	0.066(0.016)	0.195(0.005)	UBVRIJH
SN2005na	0.79	0.24	0.061(0.022)	0.068(0.003)	UBVRI
SN2005eq	0.73	0.2	0.044(0.024)	0.063(0.003)	UBVRIJH
SN2005M	0.76	0.08	0.060(0.021)	0.027(0.002)	UBVRIJH
SN2007on	0.3	0.09	< 0.007	0.010(0.001)	UBVRIJH
SN2007nq	0.58	0.17	0.046(0.013)	0.031(0.001)	BVRI
SN2005am	0.48	0.2	0.053(0.017)	0.043(0.002)	UBVRIJH
SN2005hc	0.8	0.2	0.049(0.019)	0.028(0.001)	UBVRIJH
SN2004gu	0.74	0.15	0.096(0.034)	0.022(0.001)	BVRI
SN2011fe	0.52	0.15	0.03(0.01)	0.021(0.001)	UBVRIJH
SN2001ba	0.58	0.15	0.06(0.02)	0.08 (0.002)	UBVRIJH
SN2002dj	0.64	0.26	0.04(0.03)	0.06 (0.003)	UBVRIJH
SN2002fk	0.74	0.23	0.07(0.02)	0.02 (0.003)	UBVRIJH
SN2008R	0.25	0.1	0.009(0.013)	0.062(0.001)	UBVRIJH
SN2005iq	0.52	0.11	0.040(0.015)	0.019(0.001)	UBVRIJH
SN2005ki	0.51	0.27	0.016(0.013)	0.027(0.001)	UBVRIJH
SN2006bh	0.42	0.15	0.037(0.013)	0.023(0.001)	UBVRIJH
SN2007bd	0.6	0.13	0.058(0.022)	0.029(0.001)	UBVRIJH

Table 2. L_{max} measurements for low reddening SNIa with a measured t_2.

SN	L_{max}	e_L	$M_{Ni}-Arn$	$M_{Ni}-DDC$
SN2008gp	1.29	0.14		
SN2007as	0.81	0.05		
SN2008bc	1.32	0.19		
SN2008hv	1.08	0.13		
SN2008ia	1.13	0.14		
SN2005na	1.42	0.24		
SN2005eq	1.32	0.2		
SN2005M	1.37	0.08		
SN2007on	0.6	0.09		
SN2007nq	0.91	0.17		
SN2005am	1.1	0.2		
SN2005hc	1.46	0.2		
SN2004gu	1.30	0.15		
SN2011fe	1.1	0.15		
SN2001ba	1.18	0.15		
SN2002dj	1.25	0.26		
SN2002fk	1.42	0.23		
SN2008R	0.53	0.1		
SN2005iq	1.07	0.11		
SN2005ki	1.03	0.27		
SN2006bh	0.86	0.15		
SN2007bd	1.22	0.13		

$$L_{Max} = 0.033(\pm 0.009) * t_2(H) - 0.239(\pm 0.203) \quad (1c)$$

The scatter around the best fit in YJH bands is 0.18, 0.16 and 0.22 (* $e^{43} ergs^{-1}$) respectively. This reflects the strength of the correlations in the individual bands

From the sample presented in Table 2, we reject objects with a total E(B-V) (host galaxy + MW) of $\geq$ 0.1. As a result, 7 objects with $E(B-V)_{host}$ <0.1 but total E(B-V) $\geq$ are removed. We do not find a substantial decrease in the correlation coefficients in the YJH bands. Since we know the reddening law in the MW, which allows us to correct for the absorption by dust, we include these objects in our analysis to have as large a sample as possible.

Equations (**??**) relate the timing of the second maximum to the peak bolometric luminosity by combining equation (**??**) with equation (**??**). We can see that the relation is dependent on the rise time of the SN and the α parameter which encodes the deviation from Arnett's rule.

From the equations it is evident that the timing of the second maximum in H doesn't provide stringent constraints on the bolometric peak luminosity.

Table 3. M_{Ni} estimates for 5 objects with high values of $E(B-V)_{host}$. We present constraints from the relation using only $t_2(J)$ as well as from both $t_2(Y)$ and $t_2(J)$. We can see a marked decrease in the error values when combined constraints are used

SN	M_{Ni} (inferred)	σ	Method
SN1986G	0.23	0.12	J band relation
–	0.25	0.07	combined fit
SN2005A	0.54	0.15	J band relation
–	0.56	0.07	combined fit
SN2006X	0.57	0.13	J band relation
–	0.57	0.07	combined fit
SN2008fp	0.63	0.15	J band relation
–	0.65	0.07	cf
SN2014J	0.58	0.23	J band relation
–	0.59	0.17	combined fit

4.2. Test Case for SN2014J and SN2006X

Using the correlations derived above, we want to estimate the Ni masses of heavily reddened SNae. The first test case is the nearby SN 2014J in M82 with an $E(B-V)_{host}$ of 1.3. Current attempts to use the bolometric light curve depend on the A_V value used and vary by a factor of ~ 2 (0.37 $M_\odot$ if using A_V=1.7 mag from **?**, compared to 0.77 using a higher A_V of 2.5 mag from **?**). In our analyses the aim is to estimate the M_{Ni} independent of the extinction.

The proximity of SN2014J, has allowed for the first γ ray Co line detection in an SNIa (Churazov+ 2014). the authors, using a line photon escape fraction from the models, deduce an Ni mass of 0.62 $\pm$ 0.13 $M_\odot$. This measurement is independent of the A_V value used and is one method of obtaining M_{Ni} for highly reddened objects. However, γ ray detections aren't possible for farther away SN, for which we require a different estimation method.

Using the best fit relation for the sample defined above , we obtain M_{Ni} of 0.57 $\pm$ 0.21 $M_\odot$ for a t_2 of 28.37 $\pm$ 5.7 days. Thus, we find a very good correspondence between the values from the γ rays and the NIR second maximum. This adds evidence to the argument that the NIR can be used for estimate M_{Ni} for highly reddened SN, even in more distant objects for which γ ray Co line detections are not possible This uncertainty in M_{Ni} can be reduced with a more precise estimate of t_2.

For SN2014J, we can get a precise measurement of the extinction from IR spectra at $\sim$ +300 days. This is again not possible for objects farther away. Thus, we apply this relation to a farther away, heavily extinguished object, SN2006X. The measured value for SN2006X of $t_2(J)$ is 28.19 with an error of 0.63 days. This results in an M_{Ni} value of 0.57 $\pm$ 0.13 $M_\odot$. We can see that a smaller uncertainty in t_2 gives a more accurate measurement of M_{Ni}. We compare this value for SN2006X to that obtained using $t_2(Y)$ and obtain M_{Ni} of 0.58 $\pm$ 0.17 $M_\odot$. We find both these values consistent with each other. The slightly higher error bar on the value from $t_2(Y)$ is due to a larger error on the intercept in the best fit relation for the Y band. For both SN2014J and SN2006X, the $t_2(H)$ gives an M_{Ni} of 0.50 $\pm$ 0.26 $M_\odot$ and 0.51 $\pm$ 0.23 $M_\odot$ respectively. We can see that a weaker correlation in the H band leads to a slight offset in the M_{Ni} estimate and a larger error bar on the measurement. Hence, we conclude that using the H band to measure the M_{Ni} is not feasible

The derived value of M_{Ni} is consistent with the conclusion that SN2006X is a 'normal' SNIa (**??**).

We include three more objects in the highly reddened sample, namely, 1986G, 2005A and 2008fp. We calculate the M_{Ni} for these objects in the same way as for SN2014J and SN2006X. We summarise our findings in Table **??**. We can see that 1986G has a lower value of M_{Ni} than the other objects in the sample. This is consistent with the observed optical decline rate and lower B band luminosity of the SN. Since we find that t_2 in both Y and J bands correlates very strongly with the M_{Ni}, we use combined constraints from the relations to obtain an M_{Ni} estimate. We can see from Table **??** that the error on the M_{Ni} reduces when using combined constraints. For 2014J, it is 0.17 $M_\odot$ whereas for the others it is much lower at 0.07 $M_\odot$

Hence, we conclude that the NIR second maximum timing (in Y and J) is a very good indicator of the amount of Nickel synthesised in the explosion, even for heavily reddened objects.

4.3. Deriving M_{Ni} from L_{max}

In the sections above, we have found a strong correlation between the peak bolometric luminosity (L_{max}) and t_2 in the Y and J bands.

Since our final aim is to derive a value of the Nickel mass for objects which have a measured value of t_2, we present the different methods to derive M_{Ni} from the peak bolometric luminosity.

4.3.1. Arnett's rule with a variable rise time

Arnett's rule states that the luminosity of the SN at peak is given by the instantaneous rate of energy deposition from radioactive decays inside the expanding ejecta. This is summarized in equation (**??**).

$$L_{max} = \alpha E_{Ni}(t_R) \tag{2}$$

Where E_{Ni} is the input from ^{56}Ni decay at maximum, t_R is the rise time and α accounts for deviations from Arnett's Rule.

$$0.040(\pm0.005)*t_2(Y)-0.055(\pm0.125)E_{Ni}(1M_\odot) = 6.45X10^{43}e^{-t_R/} \tag{3}$$

For estimates using different rise times, we follow the relation in **?**

$$t_{R,B} = 17.5 + 5(\Delta m_{15} - 1.1) \tag{4}$$

and

$$t_{R,Bol} = t_{R,B} + (t_{max,bol} - t_{max,B}) \tag{5}$$

which implies

$$L_{max} = \alpha*(6.45X10^{43}e^{-((17.5+5(\Delta m_{15}-1.1)+t_{max,bol}-t_{max,B}))/8.8}+ 1.45X10^{43}e^{-(17.5+5(\Delta m_{15}-1.1)+t_{max,bol}-t_{max,B}))/111.3})*(M_{Ni}/M_\odot) \tag{6}$$

substituting the relation derived between L_{max} and t_2 we get a relation between t_2 and M_{Ni}

$$(M_{Ni}/M_\odot) = (0.040(\pm0.005) * t_2(Y) - 0.055(\pm0.125))/ (\alpha * (6.45X10^{43}e^{-((17.5+5(\Delta m_{15}-1.1)+t_{max,bol}-t_{max,B}))/8.8}+ 1.45X10^{43}e^{-(17.5+5(\Delta m_{15}-1.1)+t_{max,bol}-t_{max,B}))/111.3}) \tag{7a}$$

$$(M_{Ni}/M_\odot) = (0.042(\pm0.004) * t_2(J) - 0.039(\pm0.102))/ (\alpha * (6.45X10^{43}e^{-((17.5+5(\Delta m_{15}-1.1)+t_{max,bol}-t_{max,B}))/8.8}+ 1.45X10^{43}e^{-(17.5+5(\Delta m_{15}-1.1)+t_{max,bol}-t_{max,B}))/111.3}) \tag{7b}$$

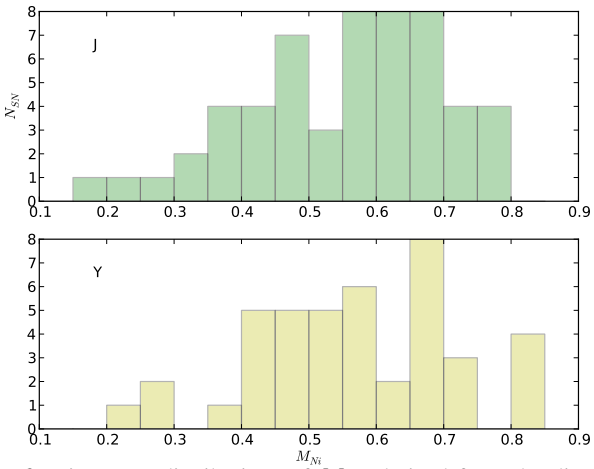

Figure 2. Histogram distributions of M_{Ni} derived from the distributions of t_2 for a complete sample of SNIa with measured t_2. This uses the Arnett's rule derivation with fixed

$$(M_{Ni}/M_{\odot}) = (0.033(\pm 0.009) * t_2(H) - 0.239(\pm 0.203))/ (\alpha * (6.45X10^{43} e^{-((17.5+5(\Delta m_{15}-1.1)+t_{max,bol}-t_{max,B}))/8.8} + 1.45X10^{43} e^{-(17.5+5(\Delta m_{15}-1.1)+t_{max,bol}-t_{max,B}))/111.3}) \quad (7c)$$

Since the Δm_{15} values are related very strongly to t_2 in the different bands, using a variable rise time leads to a non-linear relation between t_2 and M_{Ni}

4.3.2. Arnett's rule with a fixed rise time

For this method of deriving M_{Ni} from L_{max}, we use a fixed rise time of 19 days, as in **?**. Similar to their analysis, we propagate an uncertainty of $\pm$ 3 days

$$L_{max} = (2.0 \pm 0.3)X10^{43}(M_{Ni}/M_{\odot}) ergs^{-1} \quad (8)$$

For deriving equation (**??**), we use α=1.

4.3.3. Interpolating using DDC models

From these bolometric light curves, we derive M_{Ni} values by interpolating the relation between $L_{bol}(max)$ and M_{Ni} from the DDC models of **?** For objects without NIR coverage near maximum, we interpolate the values for the synthetic pseudo-bolometric light curves calculated only using the UBVRI filters. For SN2004gu and SN2007nq, which only has near maximum coverage in the $BVRI$ filters, we use the model value for only that set of filters.

4.4. Complete NIR Sample

Since we have derived the relation between L_{max} and t_2 and have presented the different ways to obtain the M_{Ni} from the L_{max}, we can then use the distribution of t_2 for all objects, independent of reddening to obtain a distribution of M_{Ni} using the relations derived

From figure **??**, we find a large scatter in the M_{Ni} values. We find that the objects vary by a factor of 3 in their M_{Ni} distribution. We note, however, that since 91bg-like objects do not show a second maximum, we do not have values in the figure $\lesssim$ 0.2 $M_{\odot}$

4.5. Comparison with published values

We searched the literature for published values of M_{Ni} for objects in our sample. In **?** , the authors published values of M_{Ni} for 2005el and 2011fe. For 2011fe, we find M_{Ni} of 0.52 $\pm$ 0.15 $M_{\odot}$ whereas the value in S14 is 0.42 $\pm$ 0.08. We note that the value of α in their study is 1.2 whereas we use α=1. Using their value of α, we find M_{Ni}= 0.44 $M_{\odot}$, which is a better agreement.

For SN2005el we find M_{Ni} of 0.44 $\pm$ $M_{\odot}$. **?** provides a discussion of this object, which in their sample they measure to have an M_{Ni} of 0.52. It is one of two outliers in their M_{Ni}-Δm_{15}. They argue that it is likely for the SN to have a lower M_{Ni} that their fiducial analysis suggests.

4.6. Bolometric Light Curve Shape

Recent studies have shown that SNIa have remarkable uniformity in the late decline rate in NIR (YJH bands). Studies like (**???**) have shown that the late declines in the optical are very uniform as well, which indicates that the SNae have a similar structure of their ejecta. **?** found a very late decline for the pseudo-bolometric light curves in their sample, with a mean decline rate of 2.6 mag per 100 days. We investigate the distribution of the exponential decline for objects in our sample.

We compute the decline rate of the pseudo-bolometric light curve between +40 and +90 days (measured with respect to B_{max}, however, we note that the value doesn't change significantly for phase measured wrt. bolometric maximum). We find a very uniform distribution of m for our objects, with $\overline{m}$=0.031 mag/day σ=0.0032. we note here that the decline rate calculated for our sample include YJH band late time data, which has been seen to have a signifcantly faster decline than the optical (0.05 mag/day compared to $\sim$ 0.01 mag/day in the optical). This explains why the average decline at late times is greater than the average for the C00 sample. For our objects we calculate the late decline in the BVRI pseudo-bolometric light curves to compare to the sample mean for C00. We find that $\overline{m}$ is 2.62 mag per 100 days with a scatter of 0.23 mag/day about the mean.

This is consistent with the findings of **?**. We look at the 91bg-likes with sufficient late time coverage in our sample and find that they have a slightly faster late decline rate and the scatter is higher than for normal Ia's.

We investigate the near peak bolometric decline (parametrized as $\Delta m_{15}(bol)$) for our sample and find a small dispersion within the sample, similar to the findings of **?**. The scatter for the complete sample is 0.18 mag for $\Delta m_{15}(bol)$, compared to the larger dispersion in Δm_{15} from the SN(oo)Py fit of 0.30 mag. This is comparable to the dispersion found in the C00 sample.

5. Discussion and Conclusion

In our sample, we observe a strong correlation between the M_{Ni} and t_2 in Y and J, and less so in the H band. This provides us with direct evidence that the timing of the second maximum is governed by the amount of Nickel produced by the supernova since it leads to a later ionization transition of the iron group elements at late time (mainly, ^{56}Co) from doubly to singly ionized (**?**).

This trend is confirmed by a strong correlation between t_L and M_{Ni} indicating that objects with more Ni produced have a slower rate of reddening and the Fe and Co lines appear later in the spectrum, which delays the onset of the lira law phase, and also the second maximum.

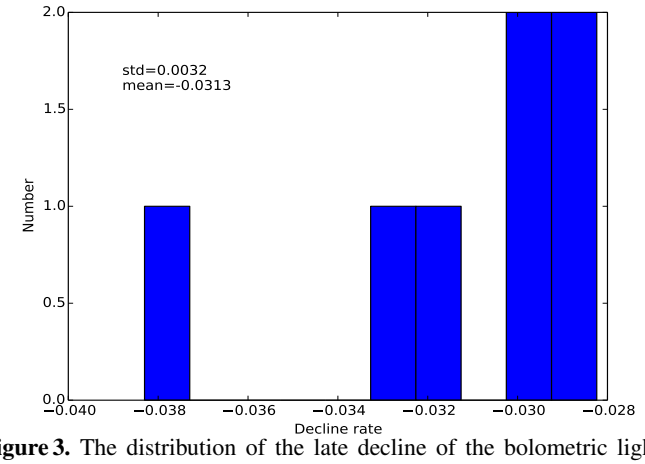

Figure 3. The distribution of the late decline of the bolometric light curve (in magnitudes per day) for our sample of objects with sufficient coverage at late epochs (see text). We observe a very small scatter in the sample

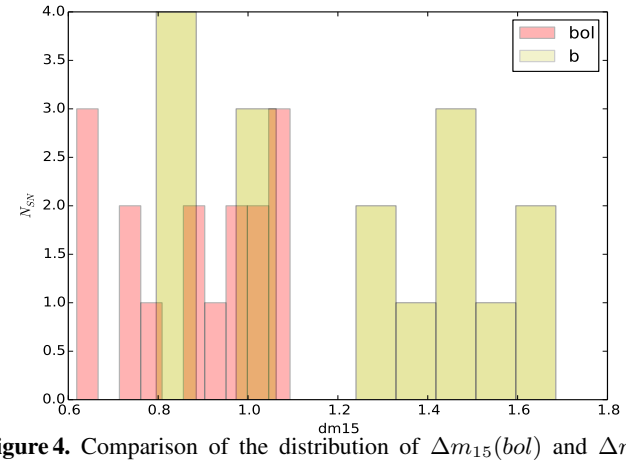

Figure 4. Comparison of the distribution of $\Delta m_{15}(bol)$ and Δm_{15} from SN(oo)Py. We find a narrower distribution of bolometric decline. We note that our sample doesn't include objects in the Δm_{15} range between 1.0 and 1.2 since none of these objects in the data pass the reddening cut

This relation offers great insight into measuring the M_{Ni} for objects not in the low-reddening sample, but with extensive NIR data. A striking example of this application is the nearby SN2014J in M82, which is heavily occluded by host galaxy dust. Since this prevents an accurate measurement of M_{Ni} from the bolometric light curves and there is a large disparity in the different values published in the literature using this method, we use the relations we obtain to constrain the M_{Ni}. For SN2014J, we have a unique opportunity to compare different estimation methods, since its proximity has allowed γ ray Co line detection and therefore, another extinction independent measurement of the M_{Ni}. Our value of 0.58 $\pm$ 0.21 M_{odot} compares very well with **?**, who find M_{Ni} of 0.61 $\pm$ 0.13 M_{odot}. The brightness of SN2014J at late times, due to its proximity, permits us to obtain NIR spectra at $\sim$ 300 days, which can provide an accurate measurement of the extinction and therefore, an accurate M_{Ni} from the bolometric light curve. This presents us with a confrontation of several different methods to measure the M_{Ni} and hence obtain a conclusive estimate on the amount of Ni produce in this SN.

Since γ detections are unlikely for farther out SN and most of them are too faint at $\sim$ +300 days for IR spectroscopy, we apply our method to other heavily reddened SN that are farther away than SN2014J. The first object we analyse is SN2006X. From the measurement of 0.57 $\pm$ 0.15 M_{odot}, we conclude that 2006X produced the average amount of Ni for an SNIa.

We also analyse the bolometric light curves at peak and during the late phase of exponential decline. We find that the SN in our sample have a uniform late time bolometric decline rate, indicating that the internal structure of the ejecta is similar for most SN. This confirms the deductions from the optical and NIR light curves in previous studies and from the bolometric light curves in sample of C00. We also find that the bolometric light curves, unlike the optical light curves, have a narrow distribution of the Δm_{15} parameter.

We conclude from our findings that there is a strong dependence of the t_2 and the colour evolution (parametrized by t_L) on the M_{Ni}

6. To add

1. t_l versus M_{Ni} plot

2. $M|_{55}$ versus Ni mass in all 3 filters

3. add columns to table 2 with t2 values so that all params are in one set.

4. possibly add ejecta masses too, depending on the point the paper is making

Acknowledgements. This research was supported by the DFG cluster of excellence Origin and Structure of the Universe' We would like to thank Chris Burns for his help with template fitting using SNooPy, Richard Scalzo for discussion on the nickel masses and Saraubh Jha on the nature of Type Ia supernovae. We thank Stephane Blondin for his comments on the manuscript. B.L. acknowledges support for this work by the Deutsche Forschungsgemeinschaft through TRR33, The Dark Universe and the Mount Stromlo Observatory for a Distinguished Visitorship during which most of this publication was prepared.